Synthesis of Polystyrene/Poly(butyl acrylate) Core–Shell Latex and Its Surface Morphology

Sang Hern Kim,[1] Won Keun Son,[1] Yong Joo Kim,[1] Eu-Gene Kang,[1] Dong-Won Kim,[1] Chang Woo Park,[1] Whan-Gi Kim,[2] Hyung-Joong Kim[3]

[1]*Department of Chemical Technology, Hanbat National University, Dukmyung-dong, Yusung-ku, Taejon 305-719, South Korea*
[2]*Department of Applied Chemistry, Kon-kuk University, Chungbuk, 380-701, South Korea*
[3]*Department of Advanced Materals, Kongju University, Chungnam, 314-701, South Korea*

Received 13 July 2001; accepted 22 April 2002
Published 11 February 2003 in Wiley InterScience (www.interscience.wiley.com). DOI 10.1002/app.11495

ABSTRACT: A polystyrene (PS)/poly(butyl acrylate) (PBA) composite emulsion was produced by seeded emulsion polymerization of butyl acrylate (BA) with PS seed particles which were prepared by emulsifier-free polymerization of styrene with potassium persulfate (KPS) under a nitrogen atmosphere at 70°C for 24 h with stirring at 60 rpm and swelled with the BA monomer in an ethanol/water medium. The structure of the PS/PBA composite particles was confirmed by the presence of the characteristic absorption band attributed to PS and PBA from FTIR spectra. The particles for pure PS and PS/PBA with a low content of the BA monomer were almost spherical and regular. As the BA monomer content was increased, the particle size of the PS/PBA composite particles became larger, and more golf ball-like particles were produced. The surface morphology of the PS/PBA composite particles was investigated by AFM and SEM. The T_g's attributed to PS and PBA in the PS/PBA composite particles were found at 110 and −49°C, respectively. The thermal degradation of the pure PS and PS/PBA composite particles occurred in one and two steps, respectively. With an increasing amount of PBA, the initial thermal decomposition temperature increased. On the contrary the residual weight at 450°C decreased with an increasing amount of PBA. © 2003 Wiley Periodicals, Inc. J Appl Polym Sci 88: 595–601, 2003

Key words: polystyrene; surface; morphology; thermal properties

INTRODUCTION

Recently, many researchers have studied the functional materials of polymers. They considered that one of the most promising methods to use is a multicomponent system with two or more polymeric components. Blending of polymers for obtaining improved properties requires the compatibility between two or more polymers. We frequently encounter the problem of blending two or more polymeric components. Therefore, there is great interest in composite emulsion polymerization for improving polymer properties. Emulsion polymerization has been used extensively in industry to prepare a wide range of polymers. Compared to bulk processes, it has the advantage that more conventional equipment can be used and much higher concentrations can be handled than in solution polymerization. One disadvantage is the relatively large amount of surfactants required.[1–4]

Micron-size monodisperse polymer particles are relevant to biomedicine, the information technology industry, microelectronics, etc. Since the micron size is between the diameter ranges of particles produced by emulsion polymerization (about 0.1–0.7 μ) and that of beads produced by suspension polymerization (about 100–1000 μ), it has been difficult to produce micron-size monodisperse particles. However, Corner[5] and Almog et al.[6] suggested that dispersion polymerization is useful for this, and other groups later recognized its usefulness.[7–9] On the other hand, Eshuis et al. and Ugelstad et al. showed that seeded polymerization utilizing a two-step swelling process with a swelling agent is useful for the purpose. The swelling agent, which is absorbed into the polymer seed particles in the first step, stimulates the swelling with a large amount of monomer in the second step.[10,11] Okubo et al. suggested a new type of swelling method of polymer seed particles with a large amount of a hydrophobic monomer and an oil-soluble initiator, separated continuously from an ethanol/water medium by a slow dropwise addition of water, being absorbed by the polymer seed particles.[12,13]

Core–shell latexes are composite particles composed of a core of one polymer engulfed in a shell of a second polymer. Composite polymer particles comprising two or more kinds of homopolymer or copolymer constituents prepared by seeded or multistage emulsion polymerization can display a wide range of properties because of their various phase morphological features and compositions. In past decades, nu-

Correspondence to: S. H. Kim.
Contract grant sponsor: Hanbat National University.

merous investigations have been published to reveal the phase structure of composite polymer particles and the relationship between the properties and their morphology.[14–16]

In general, composite polymer particles with different heterogeneous structures are formed according to their polymerization process and the properties of monomers. It has been shown that the morphology of emulsion particles is affected by the relative hydrophilicity of the monomers, the particle size of the seed polymer emulsion, the sequence and the pathway of addition of the second monomer, and the kind of initiator. Many techniques can be used to examine the morphology of composite polymer particles, which concern the direct observation by electron microscopy[17] as well as indirect methods such as dynamic mechanical spectroscopy,[18,19] soap titration,[20] and film-forming behavior.[21]

In the present article, a polystyrene (PS)/poly(butyl acrylate) (PBA) composite emulsion was produced by seeded emulsion polymerization of butyl acrylate (BA) with PS seed particles. The PS seed particles were prepared by emulsifier-free polymerization of styrene with KPS under a nitrogen atmosphere at 70°C for 24 h with stirring at 60 rpm and swelled with the BA monomer in an ethanol/water medium. The morphology, particle size, and thermal property of the composite particles will be discussed.

EXPERIMENTAL

Materials

Styrene was purified by distillation under reduced pressure in a nitrogen atmosphere and stored in a refrigerator. Potassium persulfate ($K_2S_2O_8$; Yakuri Pure Chemical Co.) was used as received. BA (Aldrich Co.) was filtered though an inhibitor removal column and stored in a refrigerator before use. Acetone and ethanol of an extrapure grade were without further purification. The deionized water was filtered with an ion-exchange column.

Preparation of PS seed particles

The polymerization of styrene was carried out in a 500 mL reactor equipped with a two-bladed fan agitator, a reflux condenser, and gas inlet. Submicron-sized PS seed particles were produced by emulsifier-free emulsion polymerization of the styrene monomer (68.2 g) in an ethanol (444 g)/water (187.5 g) medium with potassium persulfate (KPS; 0.34 g) as an initiator under a nitrogen atmosphere at 70°C for 24 h with stirring at 60 rpm.

Swelling of the seed particles with the monomer

Swelling of the PS seed particles with the BA monomer was carried out as follows: The BA monomer and the PS seed dispersion (solid content of PS: 16.82%, ethanol/water = 80/20, v/v) were charged into a 50-mL glass beaker. The mixture had been stored in a refrigerator at 0 °C for 48 h before it was reacted.

TABLE I
Preparation of PS/PBA (9/1 and 7/3, w/w) Composite Particles Produced by Seeded Emulsion Polymerization at 70°C for 24 h Under Nitrogen Atmosphere

	PS/PBA (w/w)	
Ingredient	9/1	7/3
PS seed (g)	6.003	6.003
BMA (g)	0.667	2.521
KPS (g)	0.2	0.2
Ethanol (g)	40.3	40.3
Water (g)	160.12	160.12
NaHCO3	0.3	0.3

Seeded emulsion polymerization

The seeded emulsion polymerization of BA with the PS seed particles was carried out in a 500 mL reactor equipped with a two-bladed fan agitator, a reflux condenser, and gas inlet. A PS/PBA composite emulsion was produced by emulsifier-free emulsion polymerization to the PS seed particles swelled with the BA monomer in an ethanol/water medium under a nitrogen atmosphere. PS/PBA composite particles with different compositions were produced with the KPS initiator at 70°C for 24 h with stirring at 60 rpm under the conditions listed in Table I.

FTIR spectrum

The samples used for the FTIR studies were prepared with repeated centrifugation to remove the unreacted monomer. The infrared spectra of the PS and PS/PBA composite particles were obtained from a KBr pellet using an FTIR spectrophotometer (Model AVATAR 360 FTIR, Nicolet Co.) and recorded in the absorption mode, covering a range from 400 to 4000 cm^{-1}. The resolution for all spectra was 4 cm^{-1}.

Thermal analysis

The samples used for thermal analysis were prepared by removing the unreacted monomer with a centrifuge. Differential scanning calorimetry (DSC) thermograms were obtained to determine the melting temperature (T_m) for the PS and PS/PBA using a DuPont 9900 instrument. Samples were loaded in hermetically sealed aluminum pans and measurements were taken over a range of −70 to 250°C, with a heating rate of 10°C/min under a nitrogen atmosphere.

Thermogravimetric analyzer (TGA) thermograms were obtained to determine the initial thermal decom-

position temperature for the PS and PS/PBA using a DuPont 2100 instrument. The measurements of samples were taken over a range of room temperature to 650°C with a heating rate of 10°C/min under a nitrogen atmosphere.

Particle-size measurements

The data of the PS and PS/PBA particle size were obtained from a submicron particle-size analyzer (Model Nicomp 380). The sample was diluted with water to adjust the number of photons counted per second (cps).

Extraction of PBMA from PS/PBA composite particles

The medium PS/PBA dispersion was changed from ethanol/water to acetic acid by repeated centrifugation. Acetic acid dissolves PBA but does not dissolve PS at 40°C. The extraction was carried out with stirring at 40°C for 48 h.

Scanning electron morphology (SEM)

The morphology of the pure PS and PS/PBA composite particles and the PS particles extracted from PS/PBA was observed using a scanning electron microscope (JEOL JSM 6300) with a 25-kV beam in the secondary electron-imaging mode. The samples were gold-coated to prevent surface charging.

Atomic force microscopy (AFM)

Thin films were prepared by spin coating in a freshly cleaved glass plate. The film was dried for a few minutes in air at room temperature before observation by AFM. AFM measurements were obtained with a nanoscope III (Digital Instrument, Inc., Santa Barbara, CA). All measurements were made in the contact mode.

The images were recorded at a scan rate of 2.54 lines per second. To obtain typical images for the sample, the scannings were made over a large area (e.g., 25 $\times$ 25 μm). After selecting the typical area, higher magnified images were obtained in the area of 3 $\times$ 3 μm. The digital resolution of all pictures was 256 $\times$ 256 points.

RESULTS AND DISCUSSION

Synthesis of PS and PS/PBA composite particles

The FTIR spectra of PS and PS/PBA are shown in Figure 1. Figure 1(a) displays the spectrum of the PS particles. Most mono- and polynuclear aromatic compounds have three or four peaks in the region 3080–3010 cm^{-1}. Ring carbon–carbon stretching vibrations occur in the region 1625–1430 cm^{-1}. A number of weak combination and overtone bands occur in the region 2000–1650 cm^{-1}. The FTIR spectrum of PS displays characteristic absorption bands at 3082, 3059, and 3025 cm^{-1} that are attributed to C—H stretching vibrations of an aromatic compound. The absorption band attributed to a C═C stretching vibration of aromatic rings was observed at 1601 cm^{-1}. The absorption bands attributed to a —CH_2— symmetric and asymmetric stretching vibration were observed at 2848 and 2922 cm^{-1}, respectively. The absorption bands attributed to an asymmetric deformation and scissor vibration of —CH_2— groups were observed at 1452 and 1493 cm^{-1}, respectively. Figure 1(b),(c) displays spectra of PS/PBA composite particles which have the composition of 9/1 and 7/3, respectively. The FTIR spectra of the PS/PBA composite particles display the characteristic absorption band attributed to C═O stretching vibrations of BA groups at 1733 cm^{-1}. The absorption bands attributed to a C—O—C symmetric and asymmetric stretching vibration and a C—O stretching vibration of aliphatic esters were observed at 1116, 1256, and 1165 cm^{-1}, respectively. Also, the characteristic absorption bands of PS in these spectra were confirmed. These spectroscopic data indicate that the resulting polymer particle contains the PA and PBA domains.

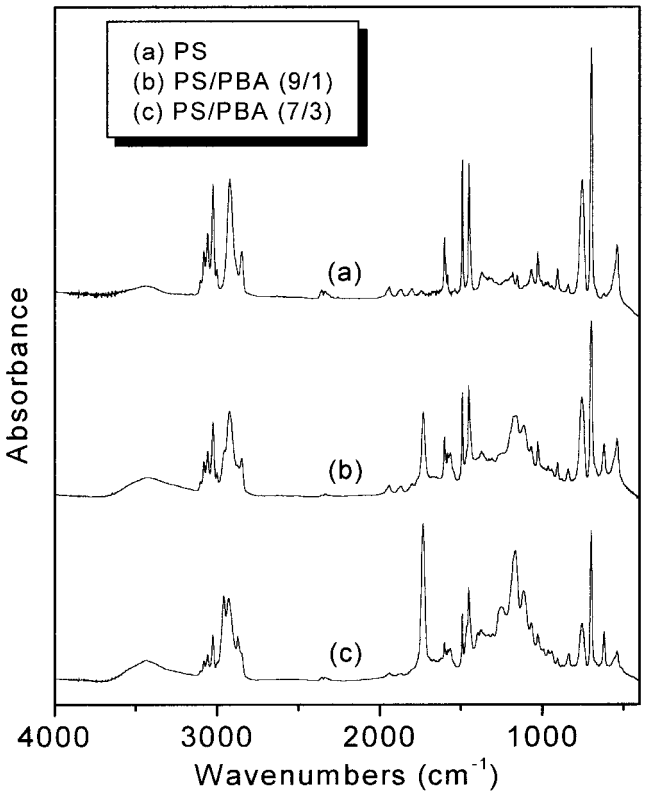

Figure 1 FTIR spectra: (a) PS particles; (b) PS/PBA composite particles (9:1); (c) PS/PBA composite particles (7:3).

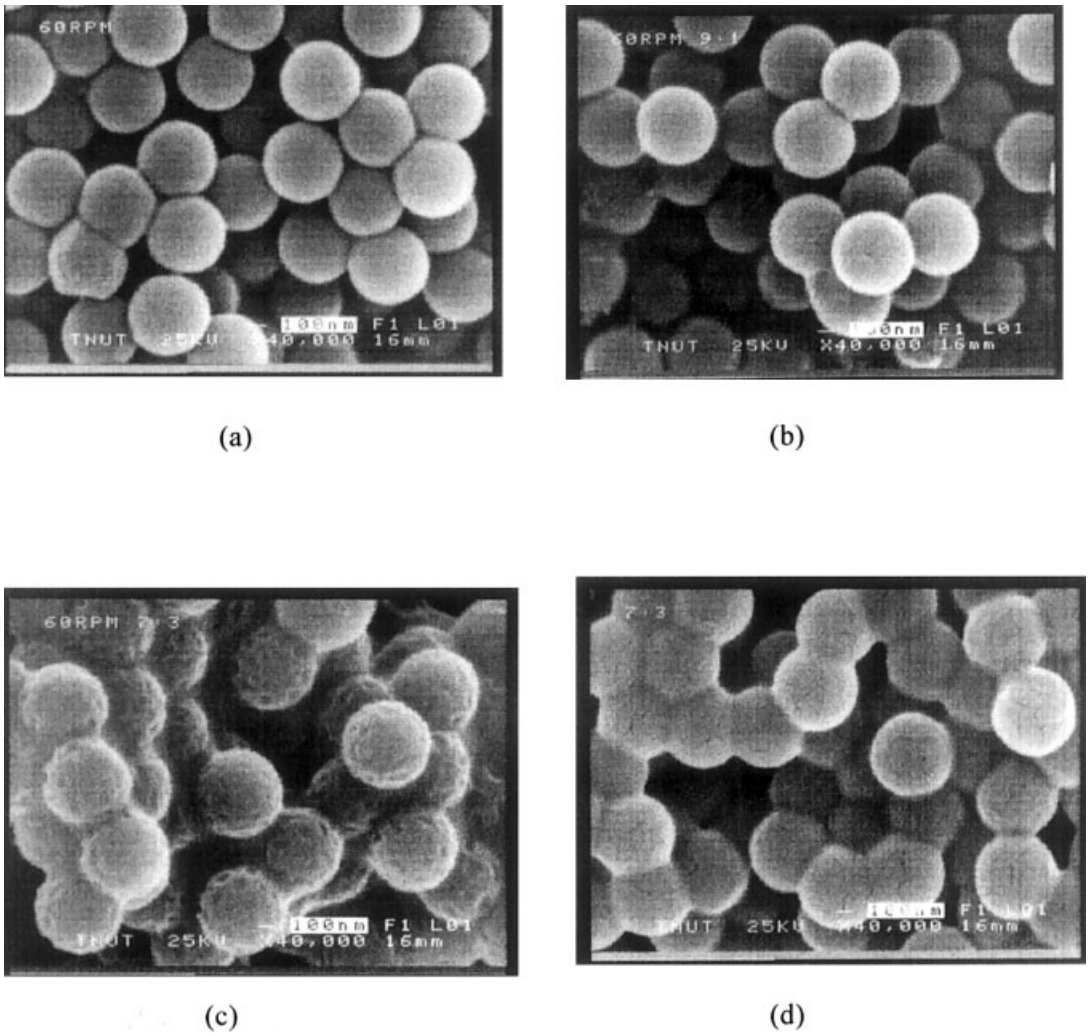

Figure 2 SEM photographs: (a) PS particles; (b) PS/PBA composite particles (9:1); (c) PS/PBA composite particles (7:3); (d) PS/PBA composite particles (7:3) after extraction with acetic acid at 40°C for 48 h.

Morphology of PS and PS/PBA composite particles

Figure 2 shows SEM photographs of the PS particles and the PS/PBA (9/1 and 7/3, w/w) composite particles produced by seeded emulsion polymerization at 70°C with the KPS initiator under a nitrogen atmosphere. Figure 2(d) shows that the PS/PBA composite particles were extracted by acetic acid. The particles of pure PS and PS/PBA with a low content of the BA monomer were almost spherical and regular. As the BA monomer content was increased, the particle size of the PS/PBA composite particles became larger and more golf ball-like particles were produced. Since the increase of BA concentration in the polymerizing particle should reduce the viscosity therein, this result suggests that the mobility of polymer molecules within the polymerizing particle is related to the formation of golf ball-like particles.

The formation mechanism of the golf ball-like particles is explained simply as follows: In the early stage of the polymerization, PBA domains are formed at the particle surface and the absorbed BA monomers in the particles are predominantly located there. As the result, a PS-rich continuous phase is always fixed because the glass transition temperature of PS is about 110°C, which is higher than the polymerization temperatures. In the polymerization system, since almost all BA monomers have been absorbed at low conversion, as the conversion of BA increases, the PBA domains swollen with the BA monomer gradually contract and result in dents at the particle surface. As shown in Figure 2(d), the shapes of the particles (PS/PBA = 7/3, w/w) after extraction by acetic acid became spherical, the same as that of the pure PS particles. Therefore, according to the above-mentioned formation mechanism, PS/PBA composite particles should be more clearly explained by the formation of a core–shell structure through seeded emulsion polymerization of BA with the PS seed particles.

Figure 3 shows AFM images of the PS particles and PS/PBA composite particles observed in the contact

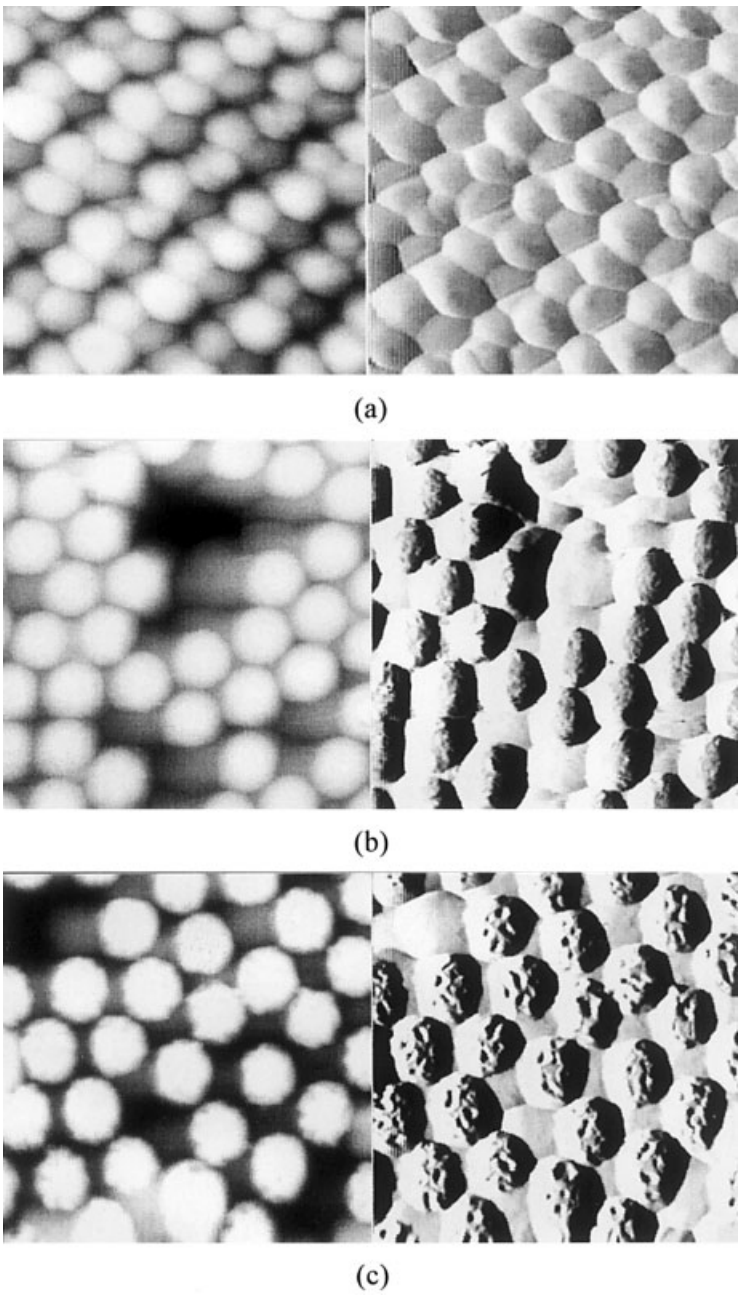

Figure 3 AFM images: (a) PS particles; (b) PS/PBA composite particles (9:1); (c) PS/PBA composite particles (7:3).

mode. The scanning dimension was 2×2 μm for all images. These images were obtained with the height (left) and deflection (right) mode. The particles of pure PS and PS/PBA with a low content of the BA monomer were almost spherical. However, it was found that the particle size of the PS/PBA (7/3, w/w) composite particles became larger, and golf ball-like particles were produced. Also, these results are the same as those of SEM.

Particle-size measurements

particle-size distributions for pure PS and PS/PBA composite particles are shown in Figure 4. As also shown in Figure 4, the particle-size distributions for pure PS and the PS/PBA composite particles were narrow. The particle size of pure PS is 541 nm and the particle size for 9/1 and 7/3 components in the PS/PBA composite particles were 578 and 680 nm, respectively. With an increasing of amount of the BA monomer, the particle size of the PS/PBA composite particles increases. The average particle size obtained from the SEM photographs, AFM images, and particle-size analyses are shown in Table II. The obtained particle sizes for pure PS and the PS/PBA composite particles from the different instruments were close to each other.

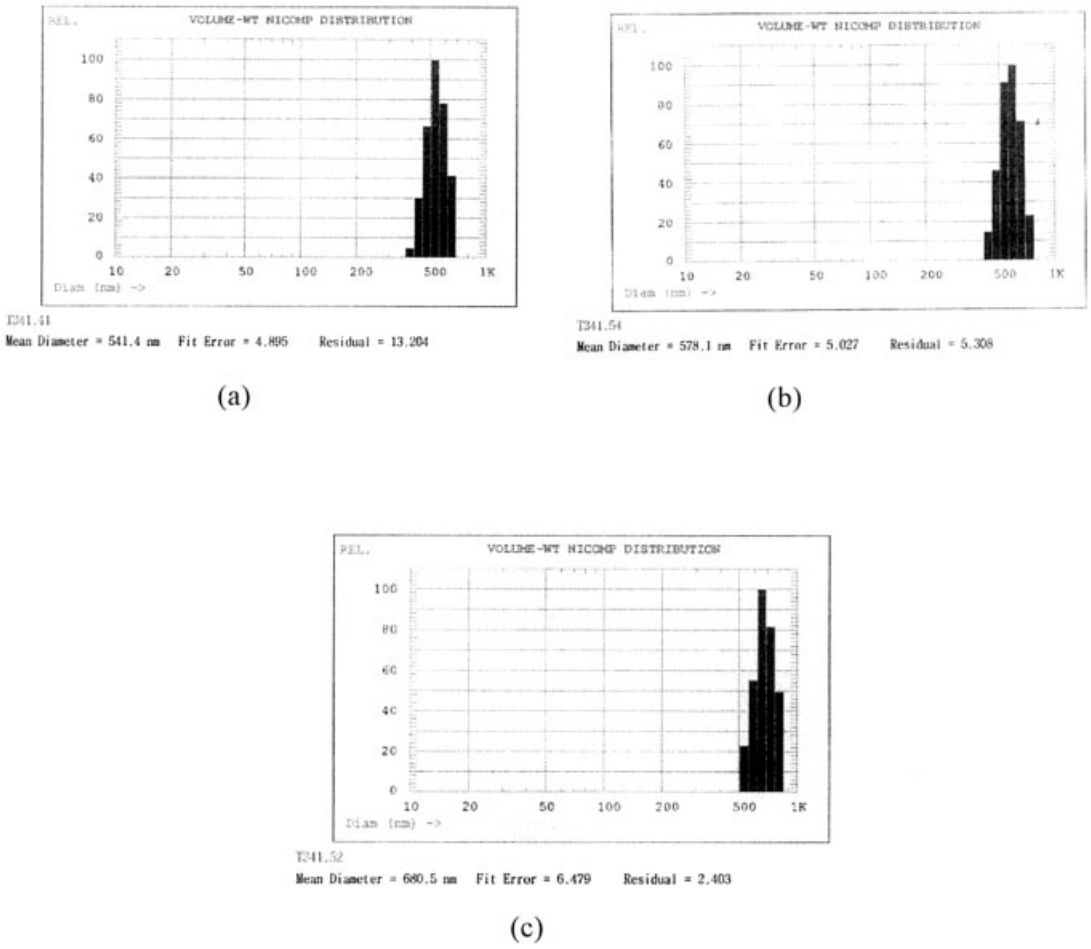

Figure 4 Particle-size distribution: (a) PS particles; (b) PS/PBA composite particles (9:1); (c) PS/PBA composite particles (7:3).

Thermal behavior

Figure 5 shows DSC thermograms for pure PS and the PS/PBA composite particles. The glass transition temperature (T_g) and melting temperature (T_m) were taken as the half-height of the corresponding heat capacity peak. As shown in Figure 5(a), the T_g of pure PS particles was found to be 110°C. The T_g and T_m for pure PBA in Figure 5(d) were observed at −49 and 45°C, respectively. The T_g's attributed to PS and PBA in the PS/PBA composite particles were found at 110°C and −49°C, respectively. These DSC thermograms indicated that composite particles contained PS

TABLE II
Average Particle-size Measured with SEM, AFM, and Submicron Particle-size Analyzer (SPS)

	Average particle size (nm)		
Instrument	PS	PS/PBA (9/1)	PS/PBA (7/3)
SEM	532	568	661
AFM	527	573	669
SPS	541	578	680

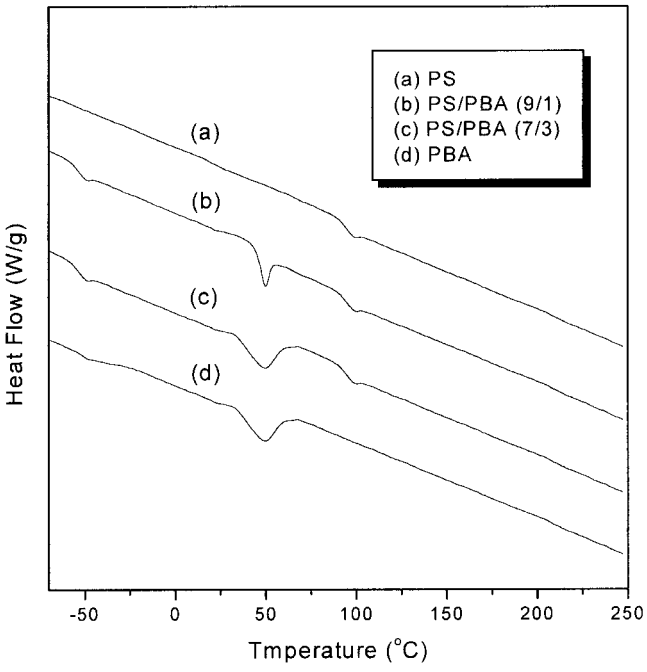

Figure 5 DSC thermograms: (a) PS particles; (b) PS/PBA composite particles (9:1); (c) PS/PBA composite particles (7:3); (d) PBA.

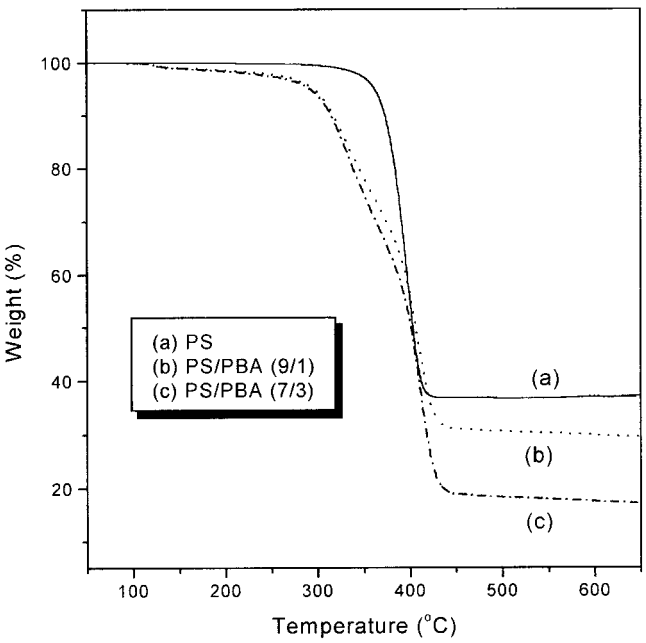

Figure 6 TGA thermograms: (a) PS particles; (b) PS/PBA composite particles (9:1); (c) PS/PBA composite particles (7:3).

and PBA domains within the polymer composite particles.

Thermogravimetric thermograms for pure PS and the PS/PBA composite particles are shown in Figure 6. The degradation of pure PS occurred in one step. PS begins to decompose at about 326°C and approximately 64% of its original weight decreased at 432°C in a nitrogen atmosphere. On the other hand, the degradation of the PS/PBA composite particles occurred in two steps. The weight losses for the 9/1 and 7/3 components at 450°C were 72 and 83%, respectively. With an increasing amount of PBA, the initial thermal decomposition temperature increased. On the contrary, the residual weight at 450°C decreased with an increasing amount of PBA.

CONCLUSIONS

We synthesized PS/PBA composite particles by emulsifier-free emulsion polymerization of PS seed particles swelled with the BA monomer in an ethanol/water medium. To observe the morphology, SEM, AFM particle-size analysis, DSC, and TGA were used. The conclusions are as follows: The FTIR spectra of the PS/PBA composite particles showed the characteristic absorption band attributed to C═O stretching vibrations of BA groups at 1733 cm^{-1} and the characteristic absorption bands attributed to C—H stretching vibrations of the aromatic compound and a —CH_2— symmetric and asymmetric stretching vibration of PS. These spectroscopic data indicate that the resulting polymer contains the PA and PBA domains. The particles of pure PS and PS/PBA with a low content of the BA monomer were almost spherical and regular. However, as the BA monomer content was increased, the particle size of the PS/PBA composite particles became larger and golf ball-like particles were produced. The results of the AFM images are the same as those of the SEM photographs. The T_g's attributed to PS and PBA in the PS/PBA composite particles were found at 110 and −49°C, respectively. The thermal degradation of pure PS and the PS/PBA composite occurred in one and two steps, respectively. With an increasing amount of PBA, the initial thermal decomposition temperature increased. On the contrary, the residual weight at 450°C decreased with an increasing amount of PBA.

This work was supported by the Hanbat National University.

References

1. Matsumoto, T.; Okubo, M.; Shibao, S. Kobunshi Ronbunshu 1976, 33, 565–574.
2. Okubo, M.; Nakano, Y.; Matsumoto, T. Kobunshi Ronbunshu, 1980, 37, 723–727.
3. Okubo, M.; Yamashita, T. Colloid Polym Sci 1997, 275, 214–219.
4. Lee, D. I.; Ishikawa, T. J Polym Sci Polym Chem Ed 1983, 21, 147–154.
5. Corner, T. Colloids Surf 1981 3, 119–129.
6. Almog, Y.; Reich, S.; Levy, M. Br Polym J 1982, 14, 131–136.
7. Ober, C. K.; Lok, K. P.; Hair, M. L. J Polym Sci Polym Lett 1985, 23, 103–108.
8. Tseng, C. M.; Lu, Y. Y.; El-Aasser, M. S.; Vanderhoff, J. W. J Polym Sci Polym Chem Ed 1986, 24, 2995–3007.
9. Okubo, M.; Ikegami, K.; Yamamoto, Y. Colloid Polym Sci 1989, 267, 193–200.
10. Eshuis, A.; Leendertse, J.; Thoenes, D. Colloid Polym Sci 1991, 269, 1086–1089.
11. Ugelstad, J.; Kaggerud, K. H.; Hansen, F. K.; Berge, A. Makromol Chem 1979, 180, 737–744.
12. Okubo, M.; Katayama, Y; Yamamoto, Y. Colloid Polym Sci 1991, 269, 217–221.
13. Okubo, M; Minami, H. Colloid Polym Sci 1997, 275, 992–997.
14. Cook, D. G.; Rudin, A.; Plumtree, A. J Appl Polym Sci 1992, 46, 1387–1393.
15. Aerdts, A. M.; de Krey, J. E: D.; Kurja, J; German, A. L. Polymer 1994, 35, 1636–1647.
16. Aerdts, A. M.; Theelen, S. J. C.; Smit, T. M. C.; German, A. L. Polymer 1994, 35, 1648–1653.
17. Narkis, M.; Talmon, Y.; Silverstein, M. Polymer 1985, 26, 1359–1364.
18. Cavaille, J. Y.; Jourdan, C.; Kong, X. Z.; Perez, J.; Pichot, C.; Guillot, J. Polymer 1986, 27, 693–702.
19. Schlund, B.; Guillot, J.; Pichot, C.; Cruz, A. Polymer 1989, 30, 1883–1894.
20. Okubo, M.; Yamada, A.; Matsumoto, T. J Polym Sci Polym Chem Ed 1980, 18, 3219–3228.
21. Devon, M. J.; Gardon, J. L.; Roberts, G.; Rudin, A. J Appl Polym Sci 1990, 39, 2119–2128.